Effect of friction-stir welding on the microstructure and mechanical properties of an Al-Mg-Si alloy

View the article online for updates and enhancements.

Effect of friction-stir welding on the microstructure and mechanical properties of an Al-Mg-Si alloy

I Vysotskiy, S Malopheyev, S Mironov and R Kaibyshev

Belgorod State University, Pobeda 85, Belgorod 308015, Russia

E-mail: malofeev@bsu.edu.ru

Abstract. In this work, sheets of an Al-Mg-Si alloy were joined by double-side friction stir welding and tempered by standard post-weld artificial aging. The combination of relatively high FSW tool rotation and welding speed with subsequent post-weld artificial aging allowed obtaining welds with high joint efficiency. However, a high sensibility of joint efficiency from FSW tool rotation speed at constant welding speed was found. In turns, the joint efficiency of the friction-stir welds for ultimate tensile strength was found to be 72% at 800 rpm and 92% at 1100 rpm, respectively. The reasons of difference in the mechanical properties of the welds are studied.

1. Introduction

Al-Mg-Si alloys are widely used in the automotive and other industries due to an attractive combination of low density, moderate strength, excellent corrosion resistance, and relatively low cost. However, the production of complex constructions from these alloys by conventional fusion welding is challenging and this essentially complicates the manufacturing of complex engineering structures. In this context, friction-stir welding (FSW), an innovative solid-state technique, appears to be very attractive for joining these materials [1–3]. The extensive research have demonstrated that FSW of Al-Mg-Si alloys involves complex precipitation phenomena, including the dissolution of particles in the stir zone and precipitation coarsening in the heat-affected zone [1–3]. Being a strong function of the weld heat input, the above effects could be efficiently controlled through welding variables, i.e. spindle rate and feed rate. In a previous study [4], for instance, the welding parameters were optimized to provide the highest cooling rate. This minimized particles coarsening in the heat-affected zone, and, thus, resulted in a relatively high joint efficiency of the produced welds. In an attempt to improve the mechanical properties of the weldments further, an alternative strategy was implemented in the present work. To suppress the precipitation phenomena at all, a relatively weld low heat input was used. To this end, the FSW trials were conducted at a relatively low spindle rate.

2. Material and experimental procedure

The program material employed in the present study was a commercial AA6061 alloy produced by direct continuous casting. The obtained ingot was homogenized, extruded at 380 °C to ~75% of area reduction and subjected to a standard T6 tempering, i.e., solutionized at 550 °C for 1h, water quenched and subsequently artificially aged at 160 °C for 8 h.

The tempered sheets were friction-stir butt welded along the extrusion direction using an AccuStir 1004 FSW machine. The welding tool was fabricated from a tool steel and consisted of a 12.5-mm-

diameter shoulder and a M5 cylindrical probe with a length of 1.9 mm. The thickness of the welding blanks was 3 mm. To provide a full-thickness joining, a double-side FSW was applied in mutually opposite directions. To investigate the effect of the weld heat input, FSW was performed at two different spindle rates, i.e. 800 rpm and 1100 rpm, whereas a constant feed rate of 760 mm/min was employed in both cases. The principal directions of the FSW geometry were denoted as the welding direction (WD), transversal direction (TD) and normal direction (ND).

To recover the mechanical properties of the welded material, the obtained joints were artificially aged at 160 °C for 8 h. To minimize a possible effect of natural aging, the post-welding treatment was performed within ~20 min after FSW.

Microstructural observations were performed mainly by electron backscatter diffraction (EBSD) technique and optical microscopy. The final surface finish was obtained by electro-polishing in a 25 pct. solution of nitric acid in methanol. EBSD analysis was conducted by using a FEI Quanta 600 field-emission-gun scanning electron microscope (FEG-SEM) equipped with TSL OIM^{TM} software. In the EBSD maps shown, the low-angle boundaries (LABs) ($2°<\theta<15°$) and the high-angle boundaries (HABs) ($\geq15°$) were depicted as red and black lines, respectively.

To evaluate broad aspects of the distribution of the microstructure within the welded material, a microhardness profile was recorded. Vickers microhardness data were obtained by applying a load of 200 g with a dwell time of 10 s by using a Wolpert 402MVD microhardness tester.

To examine mechanical properties of the weldments, transverse tensile tests were applied. The tensile specimens were centered at the weld centerline and included all characteristic microstructural zones of FSW. The tensile tests to failure were conducted at ambient temperature and a constant cross-head velocity corresponding to a nominal strain rate of 10^{-3} s^{-1} by using an Instron 5882 universal testing machine. Further experimental details were described elsewhere [4].

3. Results and discussion

3.1. Base material
The microstructure of the *base material* was dominated by coarse elongated grains with a developed substructure. The average grain size in the direction of extrusion was measured to be ~200 μm. TEM observation revealed high density of nanoscale dispersoids evenly distributed in the grain interior. As follows from the scientific literature [5,6], these particles are a mixture of needle-shaped β" precipitates with minor fraction of lath-shaped Q' precipitates. In more detail, the microstructure of the base material was described elsewhere [4].
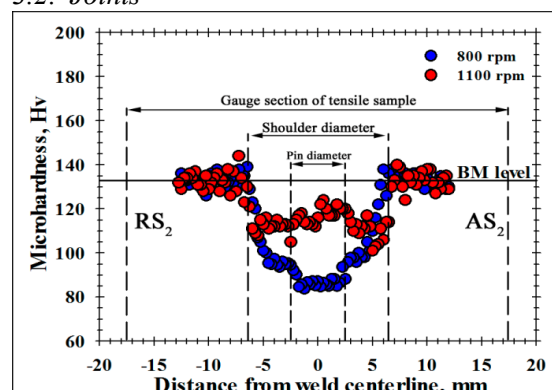
3.2. Joints

Figure 1. The microhardness profiles measured across the cross-section of the joints. Note: the horizontal solid line shows the average microhardness of the base material. RS$_2$ and AS$_2$ are retreating side and advancing side, respectively.

Microhardness profiles measured across mid-thickness of both heat-treated joints are shown in figure 1. For clarity, the shoulder- and probe diameters were indicated in the figure; the dimension of the gauge section of the tensile specimens was also shown. To a first approximation, the diameter of the shoulder indicates the region most influenced by the weld heat input. In both welds, softening of the material was found in this area. The effect was most pronounced in the weld produced at relatively low spindle rate of 800 rpm. Remarkably, the lowest strength in this case was found in the microstructural region outlined by the tool probe, i.e., virtually, in the stir zone. In contrast, the weld produced at a

relatively high spindle rate exhibited relatively high strength level with a minimal microhardness measured in the heat-affected zone, as is normally found in friction-stir welded heat-treatable aluminum alloys [1–3].

Typical EBSD grain-boundary maps taken from the central portion of stir zone of the produced joints are shown in figures 2a and b. In both cases, the microstructure was dominated by relatively-fine grains. As expected, the weld obtained at a relatively low spindle rate (i.e., a lower heat input) was characterized by a smaller mean grain size (2.8 μm vs 7.5 μm) and larger LAB fraction (38 pct. vs 18 pct.), as shown in figures 2a and b.
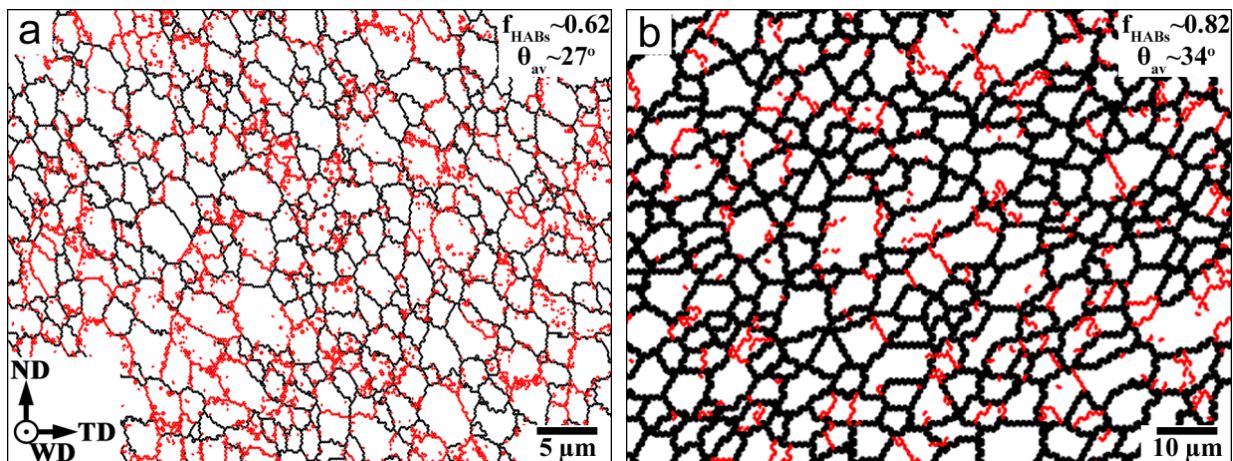

Figure 2. EBSD grain-boundary maps showing typical microstructures in the center of the stir zone of the joints produced at a spindle rate of 800 rpm (a) and 1100 rpm (b). The f_{HABs} and θ_{av} in the inserts in the top right corner are the HABs fraction and the average misorientation, respectively.

Typical deformation diagrams recorded during the transverse tensile tests of the base material and the joints are shown in figure 3. The relevant mechanical characteristics are summarized in table 1. Both welds exhibited inferior strength and ductility than the base material. Importantly, the material softening was again most pronounced in the welds produced at relatively low spindle rate and the joint efficiency in this case was only 72 pct. (table 1). In both welds, the tensile strain was found to be localized in the softened region, i.e. either in the heat affected zone in the 1100-rpm weld or in the stir zone in the 800-rpm weld (not shown).
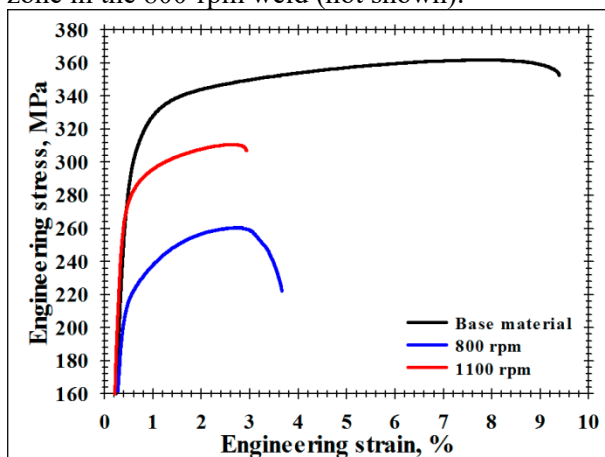

Figure 3. Typical deformation diagrams of the base material and the joints produced at a spindle rate of 800 rpm and 1100 rpm recorded during transverse tensile tests.

It is relatively well established that the strength characteristics of heat-treatable aluminum alloys are primarily governed by second-phase particles. Therefore, a clear difference in the tensile behavior between two welded materials was perhaps attributable to different precipitation behavior during FSW and the post-weld treatment. In the previous work [4], it was proposed that the peak temperature during FSW at 1100 rpm exceeded ~500 °C and that the strengthening precipitates in the stir zone completely dissolved. Accordingly, the post-weld aging resulted in nearly-full re-precipitation of the particles, thus essentially recovering the strength of the material.

On the other hand, the relatively low strength exhibited the 800-rpm weld suggests

that the particles re-precipitation in this case was incomplete. It is likely that the peak welding temperature in this case was below the solvus temperature of the particles, and therefore the microstructure evolution in this case was governed by precipitation coarsening rather than precipitation dissolution. This effect was enhanced further by the post-welding aging, and therefore the final mechanical properties of such welds were relatively low (figure 3 and table 1).

Table 1. Mechanical properties of the *base material* and the *joints*.

Material condition	Yield strength, MPa	Ultimate tensile strength, MPa	Ductility, %	Joint efficiency for UTS, %	Failure location
Base material	305	360	9	-	-
FSW at 800 rpm	220	260	3.4	72	Stir zone
FSW at 1100 rpm	280	310	2.4	92	Heat-affected zone

4. Conclusions

In the present work, the influence of the spindle rate (800 rpm and 1100 rpm) on the microstructure and mechanical properties of friction-stir welded 6061 aluminum alloy was examined.

It was found that a reduction of the spindle rate resulted in essential degradation of the weld strength. This effect was attributed to the relatively low welding temperature, which led to precipitation coarsening rather than to precipitation dissolution in the stir zone. As a result, the post-weld aging treatment was not efficient for recovering of strength of the material.

Acknowlegements

References

[1]   Threadgill P L, Leonard A J, Shercliff H R and Withers P J 2009 *Int. Mater. Rev.* **54** 49
[2]   Mishra R S, De P S and Kumar N 2014 *Friction Stir Welding and Processing* (Cham: Springer)
[3]   Mishra R S and Ma Z Y 2005 *Mater. Sci. Eng.* R *Rep.* **50** 1
[4]   Malopheyev S, Vysotskiy I, Kulitskiy V, Mironov S and Kaibyshev R 2016 *Mater. Sci. Eng.* A **662** 136
[5]   Esmaeili S, Wang X, Lloyd D J and Poole W J 2003 *Metall. Mater. Trans.* A **34** 751
[6]   Wang X, Esmaeili S, Lloyd D J 2006 *Metall. Mater. Trans.* A **37** 2691
[7]   Mironov S, Malopheyev S, Vysotskiy I, Zhemchuzhnikova D and Kaibyshev R 2018 *Defect Diffus. Forum* **385** 359